# Magnetic hyperthermia-induced drug release from ureasil-PEO-$\gamma$-Fe2O3 nanocomposites

B. L. Caetano, C. Guibert, R. Fini, J. Fresnais, S. H. Pulcinelli, C. Ménager, C. V. Santilli

Journal Name

COMMUNICATION

# Magnetic hyperthermia-induced drug release from ureasil-PEO-γ-$Fe_2O_3$ nanocomposites.

B. L. Caetano,[a,b*] C. Guibert,[b] R. Fini,[a] J.Fresnais,[b] S.H. Pulcinelli,[a] C. Ménager,[b] C. V. Santilli.[a]

**A multifunctional material suitable for cancer therapy, which combines stimuli-responsive properties for drug delivery and magnetic hyperthermia prepared by the one-pot sol-gel synthesis from the conjugation of ureasil cross-linked poly (ethylene oxide) (U-PEO) hybrid materials with the superparamagnetic nanoparticles (γ-$Fe_2O_3$), is reported in this communication.**

Organic-inorganic hybrid (OIH) materials have tremendous potential as a bridge between the organic, mineral, and biological universes, opening new frontiers for the development of systems and devices for human health care, with applications in the areas of dentistry, cosmetics, tissue engineering, therapeutic vectors, and drug delivery.[1] Among the OIH used as drug delivery vehicles, siloxane cross-linked organic macromers are an emerging option.[2] The commercially available macromer poly(ethylene oxide) (PEO), otherwise known as poly(*ethylene glycol*) (*PEG*), is approved by the FDA for parenteral administration due to its low toxicity and biocompatibility.[3] Ureasil-PEO (U-PEO) is a transparent and rubber-like OIH composed of PEO macromers of variable lengths, grafted at both ends to siloxane cross-linked nodes that are conjugated by means of urea bridges. U-PEO presents good mechanical and thermal stability[2] and exhibits hydrophilic characteristics, with water uptake resulting in swelling similar to that of hydrogels. Due to these properties, U-PEO has a high capacity to dissolve ionic species and polar molecules, and has been tested as an absorbent for water treatment[4] and as a drug delivery system. It offers efficient inclusion of high concentrations of different active molecules such as sodium diclofenac and cisplatin, for which uptake rates of 17 and 5 wt% have been reported, respectively.[2, 5] Furthermore, U–PEO hybrids prepared by the sol-gel route possess good film-forming properties (skin bioadhesion, workability, and water permeability) and have potential applications in pharmaceutical formulations for transdermal (patches) and implantable (soft tissue) drug carriers.[6] In recent work, the PEO polymer has been used in drug targeting and in stimuli-responsive drug delivery systems.[7, 8] However, there are only a few reports that have focused on the use of U-PEO hybrids as stimuli-responsive systems, and no work concerning drug delivery triggered by an external magnetic field.[9]

Magnetic nanoparticles (MNP) based on iron oxide (maghemite γ-$Fe_2O_3$ or magnetite $Fe_3O_4$) are another class of materials highly suitable for use in biomedical applications, due to their biocompatibility and superparamagnetic properties.[10, 11] Superparamagnetism is crucial for many applications in biomedicine, because when the external magnetic field is removed, superparamagnetic NP do not retain any magnetism. In addition, these MNP can be used as energy transfer mediators by transforming an external magnetic field into heat.[12] When MNP are exposed to an alternating magnetic field (AMF), the magnetic energy is dissipated as thermal energy by means of two distinct mechanisms, Néel and Brown relaxation, as the particle returns to its equilibrium state.[13] Superparamagnetic NP can therefore be used as a source of hyperthermia to cause the death of cancer cells.[14] They can also trigger drug release following application of an AMF, and can provide magnetic guidance of the drug delivery carrier to a specific target.[15] This combination of thermo- and chemotherapy can increase efficiency and reduce side effects during the treatment of radiosensitive and radioresistant tumors.[16]

There are few reports in the literature concerning ureasil–polyether hybrid systems containing MNP. However, the one-pot sol-gel synthesis method has been used to grow ferrihydrite NP in a U-PEO hybrid matrix, resulting in a non-superparamagnetic material.[17]

In this communication, we propose implantable devices that combine the drug delivery and stimuli-responsive properties of U-PEO with the superparamagnetic properties of γ-$Fe_2O_3$ NP, in order to obtain a stimuli-responsive material. To this end, we prepared an innovative multifunctional U-PEO-γ-$Fe_2O_3$ nanocomposite loaded with sodium diclofenac (SDCF) as a model drug, which under an external AMF was able to control the temperature at an optimum

[a] *Instituto de Química, UNESP, Rua Professor Francisco Degni, 55, 14800-900 Araraquara, SP, Brazil.*
[b] *Sorbonne Universités, UPMC Univ Paris 06, CNRS, Laboratoire PHENIX, Case 51, 4 place Jussieu, F-75005 Paris, France.*
[c] *Address here.*
† Footnotes relating to the title and/or authors should appear here.
Electronic Supplementary Information (ESI) available: [details of any supplementary information available should be included here]. See DOI: 10.1039/x0xx00000x

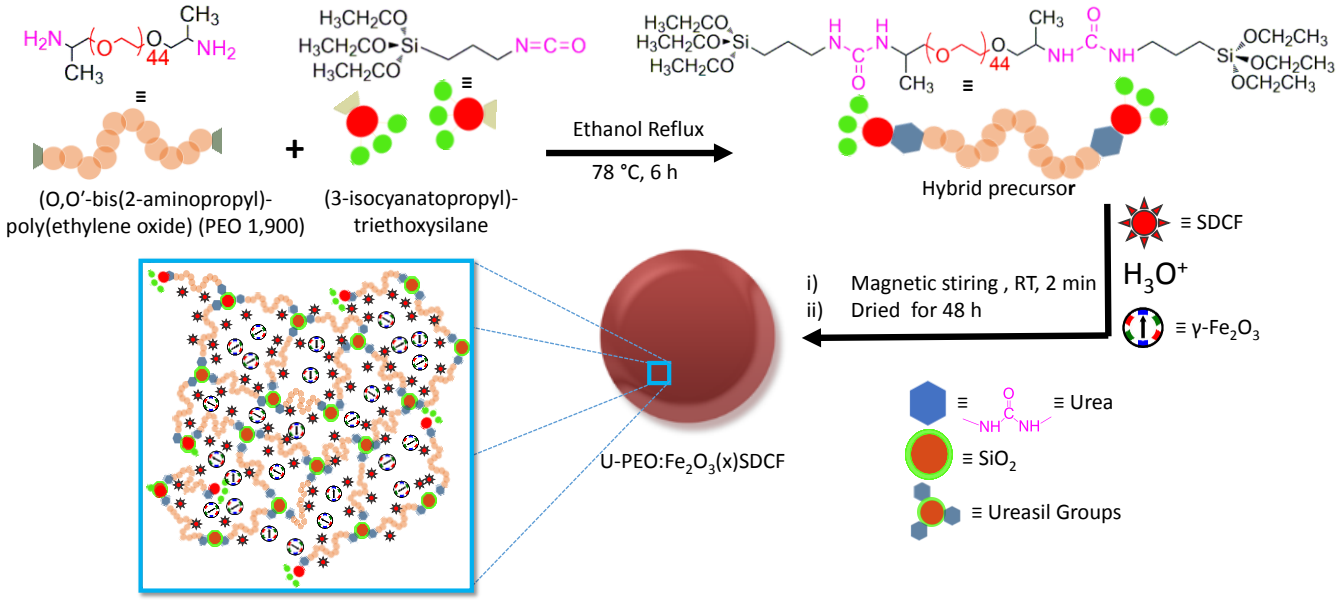


**Scheme 1** Schematic representation of the synthesis of UPEO:$Fe_2O_3$(X)SDCF nanocomposites. See more information on Supporting Information.

value for hyperthermia, as well as the drug release rate.

The samples were obtained by hydrolysis and condensation of the -Si(OEt)$_3$ groups present in the hybrid precursor (EtO)$_3$Si(CH$_2$)$_3$NHC(=O)NHCHCH$_3$CH$_2$–(PEO)–CH$_2$CH$_3$CH NH(O=))CNH(CH$_2$)Si(OEt)$_3$ with PEO1,900.[18] The hydrolysis was initiated by adding $HNO_3$ solution, followed by addition of γ-$Fe_2O_3$ NP dispersed in water at acid pH. The MNP were size-sorted at the end of the co-precipitation process in order to retrieve the larger nanoparticles that are more effective in hyperthermia.[19] In the case of the samples loaded with the model drug, 3 wt% of SDCF was added to 0.5 mL of hybrid precursor, while 5.0, 0.5, 0.05, and 0.005 wt% of γ-$Fe_2O_3$ were used in the samples containing MNP. In this work, the ureasil–poly(ethylene oxide) hybrids obtained from the precursor are labelled U-PEO, the OIH nanocomposites containing γ-$Fe_2O_3$ are labelled U-PEO:$Fe_2O_3$(x), with x being the amount (wt%) of γ-$Fe_2O_3$, and the samples loaded with γ-$Fe_2O_3$ and SDCF are denoted U-PEO:$Fe_2O_3$(x)SDCF. The experimental procedures used for synthesis and characterization are outlined in the Supporting Information (SI). The γ-$Fe_2O_3$ MNP with mean diameter ($d_o$) of 12.7 nm and polydispersity (σ) of 4.4 nm are presented in Figures 1a and 1b. Cryo-TEM images of the nanocomposite showed the absence of extensive aggregation and a fairly uniform distribution of MNP ($d_o$ = 12.0 nm, σ = 5.9 nm, Figures 1c and 1d). Using Langevin formalism weighted with a Gaussian size distribution to fit the magnetization curve (Figure 1e), $d_o$ = 0.9 nm and σ = 0.33 were obtained for the MNP in both the aqueous colloid and the OIH matrix. The $d_o$ value was in good agreement with the average size obtained by TEM, confirming the satisfactory dispersion of the MNP. It is important to note that the good dispersion of bare γ-$Fe_2O_3$ MNP was achieved by acid peptisation (pH ~1.7) of the mother suspension. In fact, the sol-gel synthesis of U-PEO:$Fe_2O_3$ should be performed at pH below 2.4 in order to maintain good dispersion of the MNP in the OIH matrix. This behaviour can be clearly seen from comparison of the SAXS curves (Figure 1f) for the nanocomposites prepared at pH ~1.7 (blue line) and pH ~3.7 (dashed line).

For the nanocomposite prepared at pH ~3.7 the SAXS curve at low q-range revealed a linear dependence, with a slope value of -1.9, evidencing the growth of fractal aggregates .[20] A weak and broad peak centred at ~0.34 nm$^{-1}$ was evidence of interaction between the MNP, due to the coexistence of dense aggregates of γ-$Fe_2O_3$. In contrast, the plateau at low q-range in the SAXS curve for the nanocomposite prepared at pH ~1.7 was characteristic of a non-interacting set of nanoparticles, reflecting good dispersion of the MNP within the matrix. The presence of well-dispersed MNP in the OIH matrix is essential for hyperthermia applications, because aggregates act to decrease the heating capacity of the MNP.[21]

After incorporation of the γ-$Fe_2O_3$ NP in the hybrid matrix, the characteristic correlation peak of regularly spaced ureasil cross-linking nodes was no longer observed.[18] This was due to the greater electronic contrast between γ-$Fe_2O_3$ and the U-PEO. It was also observed that the curves for samples containing the MNP prepared at pH ~1.7 presented similar shapes, indicating that the dispersions of MNP in the colloidal suspension and in the U-PEO hybrid with or without SDCF were comparable. The SAXS curves of the γ-$Fe_2O_3$ colloidal suspension presented a Gaussian decay in the high q region and a plateau at low q, also known as the Guinier region.

This latter feature is characteristic of scattering by a dilute set of non-interacting particles. The same behaviour could be seen for the U-PEO:$Fe_2O_3$ prepared at pH 1.7. At high q, the curves displayed an asymptotic linear trend with a slope of ~-4, in agreement with Porod's law ($I(q) \propto q^{-4}$) and implying that the two-electron density contrast model was satisfied. It also indicated that the interface between the MNP and the matrix was sharp and well-defined, with an absence of heterogeneities inside the MNP, and that each nanoparticle acted as a single object. Under such conditions, the scattering intensity in the low q region ($q.Rg \approx 1$) can be approximated by the Guinier law, enabling determination of the average gyration radius, Rg, of scattering by isolated MNP.[22] The average spherical size calculated from Rg was ~10.5 nm for both the γ-$Fe_2O_3$ aqueous colloid and the nanocomposite. These results were

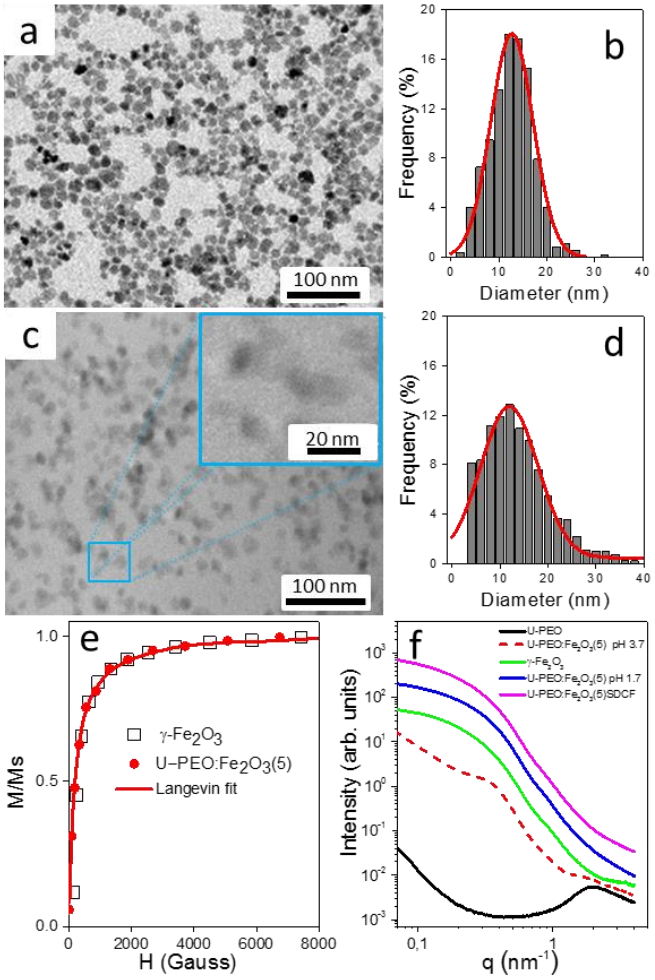


**Fig. 1** a) TEM image of $\gamma$-$Fe_2O_3$ colloid; b) Gaussian size distribution determined from TEM images of $\gamma$-$Fe_2O_3$ colloid; c) Cryo-TEM image of the U-PEO:$Fe_2O_3$(5) nanocomposite, prepared at pH ~1.7. The insert displays the zoomed image; d) Gaussian size distribution of the U-PEO:$Fe_2O_3$(5) nanocomposite; e) Magnetization curves of the 3.2 wt% $\gamma$-$Fe_2O_3$ colloid and the U-PEO:$Fe_2O_3$(5) nanocomposite, both fitted with the same Langevin function (continuous line); f) SAXS curves of the U-PEO matrix, the aqueous colloid (3.2 wt% $\gamma$-$Fe_2O_3$, pH ~1.7), and nanocomposites without (U-PEO:$Fe_2O_3$(5)) and with SDCF (U-PEO:$Fe_2O_3$(5)SDCF), prepared at pH 1.7 (continuous lines) and pH 3.7 (dashed line).

in agreement with the TEM images and confirmed the very good dispersion of the MNP in the U-PEO matrix. Magnetic hyperthermia was performed with the $\gamma$-$Fe_2O_3$ colloids and the U-PEO:$Fe_2O_3$ nanocomposite, using the same experimental procedure.

An AMF was applied to samples kept at initial temperature of 25 °C, using maximum amplitude of 14.9 kA $m^{-1}$ and a frequency of 420 kHz. Figure 2 shows images of the samples, together with the curves of temperature increase versus the $\gamma$-$Fe_2O_3$ MNP concentration, with each curve corresponding to a given AMF exposure time.

Irrespective of the nature of the sample, the isochronous curves showed a more intense increase of temperature as the concentration of $\gamma$-$Fe_2O_3$ increased, with this effect being lower for the U-PEO:$Fe_2O_3$ nanocomposites. For the aqueous colloid, the onset of heating occurred at a $\gamma$-$Fe_2O_3$ concentration of ~0.032 wt%,

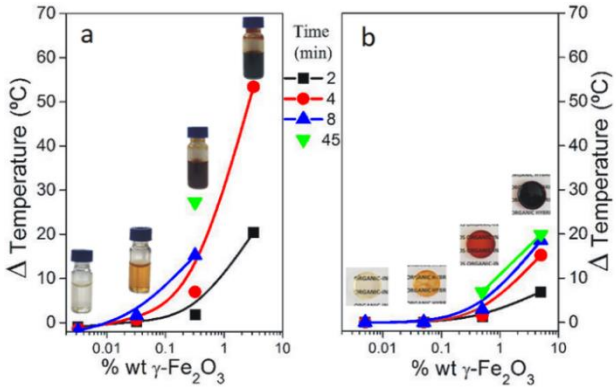


**Fig. 2** Isochronous temperature increases after application of an AMF of 14.9 kA $m^{-1}$ and 420 kHz: a) Aqueous colloid containing different amounts of MNP (3.2, 0.32, 0.032, and 0.0032 wt%); b) U-PEO:$Fe_2O_3$(x) nanocomposite containing different amounts of MNP (x = 5.0, 0.5, 0.05, and 0.005 wt%).

while for the nanocomposites, the onset of heating occurred at an MNP loading that was 15 times higher (0.5 wt% of $\gamma$-$Fe_2O_3$).

Figures 2a and 2b correspond to different concentrations of $\gamma$-$Fe_2O_3$ in aqueous colloid (3.2, 0.32, 0.032, and 0.0032 wt%) and in OIH nanocomposite (5.0, 0.5, 0.05, and 0.005 wt%), respectively. The data were obtained from monitoring of the temperature during the application of AMF (Supporting Information: Figures S1a and S1b).

As shown in Figure S1a, the colloidal suspension with 3.2 wt% of $\gamma$-$Fe_2O_3$ exhibited a prompt and continuous temperature increase, reaching 80 °C after 4 min of AMF exposure. For the ten-fold less concentrated colloid, the temperature increased continuously from 25 °C to an asymptotic value of 53 °C after 50 min of AMF exposure. In the case of the U-PEO:$Fe_2O_3$(5) nanocomposite, there was a prompt increase from 25 °C up to a stable plateau at 44 °C. For the ten-fold less concentrated nanocomposite (U-PEO:$Fe_2O_3$(0.5)), a constant temperature of 32 °C was achieved after 25 min of AMF exposure. The first 50 min of AMF exposure is shown in Figure S1b. Experiments were also performed with the same samples at a frequency of 280 kHz (Supporting Information, Figures S1c and S1d), and smaller ΔT values were observed, as expected.

The temperature plateaus indicated that the U-PEO:$Fe_2O_3$(5) and U-PEO:$Fe_2O_3$(0.5) nanocomposites were able to act as hyperthermia mediators and could be used in cancer therapy. The U-PEO:$Fe_2O_3$ nanocomposite prepared without SDCF exhibited a similar temperature increase under an AMF (data not shown). Temperatures between 40 °C and 45 °C lead to inactivation of normal cellular processes, while extensive necrosis occurs above 45 °C.[19] In the clinical application of magnetic hyperthermia, local overheating can be avoided by selecting MNP systems with low maximum achievable temperatures, while maintaining the magnetization that enables efficient local delivery.[23] For human applications, where the initial temperature is ~37 °C, an increase of 4-7 °C, as obtained using U-PEO:$Fe_2O_3$(0.5), is suitable for use in cancer therapy.

It is important to highlight that the plateau temperature was dependent on factors including the MNP concentration, the viscosity of the matrix, MNP-matrix interactions, and the rate of heat transfer to the sample holder tube. In contrast, the initial

linear rise in local temperature, $dT/dt_{max}$, (see Figure S1 and Table S1) was independent of both heat transfer to the surroundings and sample geometry, and was used to derive the specific loss power (SLP) of the nanocomposites. The SLP (W $g^{-1}$) is an intrinsic property defined as the amount of energy converted into heat per time and per mass of MNP ($m_{MNP}$): $SLP = C \cdot m_s/m_{MNP} \cdot dT/dt_{max}$ where C and $m_s$ are the specific heat capacity and the weight of the sample, respectively (see values in Table S1).[10, 14] The SLP was only calculated for the samples that showed appreciable temperature increases, with values of 97, 106, and 110 W $g^{-1}$ for the 3.2, 0.32, and 0.032 wt% $\gamma$-$Fe_2O_3$ aqueous colloids, respectively. The minor differences in SLP indicated that the degree of dispersion of the MNP was nearly invariant. In the case of the U-PEO:$Fe_2O_3$(0.5) and U-PEO:$Fe_2O_3$(5) nanocomposites, an SLP value of 13.3 W $g^{-1}$ was approximately eight-fold smaller than for the aqueous colloids. In the case of superparamagnetic particles only Néel relaxation (rotation of the magnetic moment inside the particle) is involved for heat generation. As a consequence superparamagnetic particles are not sensitive to the viscosity of the medium. In the literature, such decrease of the SLP is often explained by the formation of aggregates or strong interactions between the particles. [24] However in our case SAXS experiments prove that the particles are perfectly dispersed in the matrix. The low SLP value is probably due to the fact that we are not in adiabatic conditions, the measurement of the temperature itself is correct but the temperature elevation rate may be disturbed by temperature gradients inside the U-PEO:$Fe_2O_3$ nanocomposite.

The release of SDCF from U-PEO:$Fe_2O_3$(5):SDCF was significantly enhanced by heating either in a water bath or using an AMF (Figure 3). The release of SDCF into pH 7.2 phosphate buffer solution was performed during 8 h, at different isothermal temperatures (0, 25, 37, and 50 °C), and one additional experiment was started at 37 °C under AMF (14.9 kA $m^{-1}$, 420 kHz). The AMF was applied during ~45 min and then turned off when the temperature reached 57 °C; the temperature then returned to 37 °C after ~20 min. This cycle was repeated 8 times (see Figure S4). Irrespective of the experiment time, the amount of SDCF released followed the order: 0 °C < 25 °C < 37 °C < 50 °C ≅ AMF. This sequence can be explained by the progressive decrease of PEO crystallinity due to the relaxation induced by water uptake and the fusion that occurs near 38 °C (Fig. S5). The former process, which depends on the diffusion of water through the U-PEO matrix, is slower at low temperatures, resulting in less SDCF release. Similar release profiles were observed in experiments performed at 50 °C in a temperature-controlled water bath and under AMF, started at 37 °C. After the first hours, the cumulative drug release under AMF reached twice the value at 37 °C. The drug release rate was also significantly higher when the nanocomposites were submitted to an AMF. It could therefore be concluded that the AMF increased the diffusion rate of the drug due to fusion of crystalline domains of the U-PEO matrix following local heating. Taken together, the results supported the use of this system as a combined drug release carrier and hyperthermia source, because fusion of the semi-crystalline U-PEO resulted in a stimuli-responsive effect in the temperature range of biomedical applications.

Many of the magnetic systems used in biomedical applications rely on the key role played by the surface properties of the nanoparticles, especially in effective interfacing with biological systems, ensuring biocompatibility and specific localization in proteins, cells, and tissues.[25] These systems often use complicated

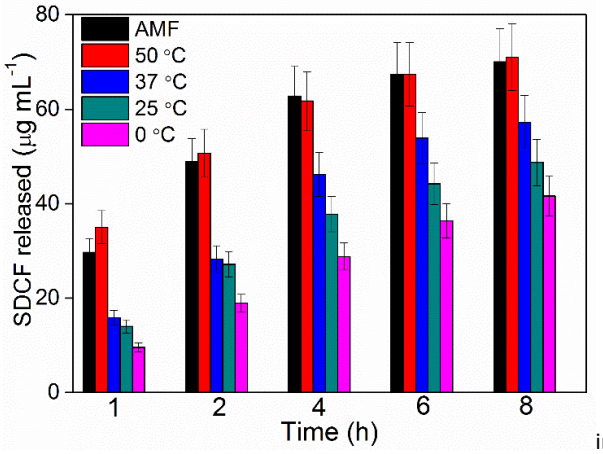


into

**Fig. 3** SDCF release from U-PEO:$Fe_2O_3$(5):SDCF at 0, 25, 37, and 50 °C, and under an external AMF started at 37 °C.

syntheses for modifying the surfaces of nanoparticles.[26] In the case of the present nanocomposites, the bare MNP were easily inserted the bulk OIH using the one-pot sol-gel synthesis, and good dispersion was achieved by controlling the pH. Furthermore, the superparamagnetic properties of the nanocomposites were quite stable, because the MNP were not leached and did not aggregate under the effects of the biological medium and the magnetic field. Another advantage of U-PEO is the ability to incorporate high amounts of drugs with different molecular natures, which can be used for specific chemotherapy,[2, 5] especially when a high dose is required in the first 2 h, after which the nanocomposite can be used continuously as a hyperthermia source. Another important consideration for in vivo applications is that the material exhibits no cytotoxic effects.[6]

In summary, this work describes the one-pot sol-gel synthesis of a nanocomposite formed by the conjugation of a semi-crystalline ureasil-poly(ethylene oxide) matrix loaded with a model drug (SDCF) and well dispersed $\gamma$-$Fe_2O_3$ superparamagnetic nanoparticles for remotely triggered therapy. Active control of the drug release rate was achieved using localised hyperthermia induced by exposure to an external AMF. The exposure caused melting of the crystalline PEO at around 38 °C, which favoured the liquid-like diffusion of drug molecules throughout the hybrid network, hence increasing the release rate. These nanocomposites show great potential for use with other drug molecules whose release can be triggered using an external magnetic field. Another very important finding was that the hybrid samples could act as mediators of hyperthermia and could therefore be used in dual cancer therapy, with hyperthermia in the optimal lower-temperature window (between 42 and 45 °C) in order to avoid thermal damage of normal cells, combined with control of the drug release profile.

This work was partially supported by the Brazilian National Council for Scientific and Technological Development (CNPq, 482176/2013-0), the Foundation for Research Support of the State of São Paulo (FAPESP, 2011/19253-0 and 2013/10384-0), and the CAPES/COFECUB-767/13 cooperation programs.

## Notes and references

1 C. Sanchez, B. Julian, P. Belleville and M. Popall, *J. Mater. Chem.*, 2005, **15**, 3559.

2 C. V. Santilli, L. A. Chiavacci, L. Lopes, S. H. Pulcinelliand A. G. Oliveira, *Chem. Mater.*, 2009, **21**, 463.
3 D. H. Na and P. P. DeLuca, *Pharm. Res*., 2005, **22**, 736.
4 V. Bekiari and P. Lianos, *Chem. Mater.*, 2006, **18**, 4142.
5 E. F. Molina, S. H. Pulcinelli, C. V. Santilli, S. p. Blanchandin and V. r. Briois, *J. Phys. Chem. B*, 2010, **114**, 3461.
6 L. K. Souza, C. H. Bruno, L. Lopes, S. H. Pulcinelli, C. V. Santilli and L. A. Chiavacci, . *Colloids Surf. B Biointerfaces*, 2013, **101**, 156.
7 X.-M. Zhang, K. Guo, L.-H. Li, S. Zhang and B.-J. Li, *J. Mater. Chem. B*, 2015, **3**, 6026.
8 A. Bin Imran, K. Esaki, H. Gotoh, T. Seki, K. Ito, Y. Sakai and Y. Takeoka, *Nature Commun.*, 2014, **5**. 1.
9 E. F. Molina, R. L. T. Parreira, E. H. De Faria, H. W. P. de Carvalho, G. F. Caramori, D. F. Coimbra, E. J. Nassar and K. J. Ciuffi, *Langmuir*, 2014, **30**, 3857.
10 N. Lee, D. Yoo, D. Ling, M. H. Cho, T. Hyeon and J. Cheon, *Chem. Rev.*, 2015, **115**, 10637.
11 A. K. Gupta and M. Gupta, *Biomaterials*, 2005, **26**, 3995.
12 R. Hergt, S. Dutz, R. Müller and M. Zeisberger, J. Phys.: *Condens. Matter*, 2006, **18**, 2019.
13 J.-P. Fortin, C. Wilhelm, J. Servais, C. Ménager, J.-C. Bacri and F. Gazeau, *J. Am. Chem. Soc*., 2007, **129**, 2628.
14 R. E. Rosensweig, *J. Magn. Magn. Mater*., 2002, **252**, 370.
15 V. S. Kalambur, B. Han, B. E. Hammer, T. W. Shield, J. C. Bischof. *Nanotechnology*, 2005, **16**, 1221.
16 J.-P. Fortin-Ripoche, M. S. Martina, F. Gazeau, C. Ménager, C. Wilhelm, J.-C. Bacri, S. Lesieur and O. Clément, *Radiology*, 2006, **239**, 415.
17 N. J. O. Silva, V. S. Amaral, V. de Zea Bermudez, S. C. Nunes, D. Ostrovskii, J. Rocha and L. D. Carlos, *J. Mater. Chem.*, 2005, **15**, 484.
18 K. Dahmouche, C. V. Santilli, S. H. Pulcinelli and A. F. Craievich, *J. Phys. Chem. B*, 1999, **103**, 4937.
19 R. Massart, *Magnetics, IEEE Trans. Magn.*, 1981, **17**, 1247.
20 T. A. Witten and L. M. Sander, *Phys. Rev. Lett*., 1981, **47**, 1400.
21 R. Di Corato, A. Espinosa, L. Lartigue, M. Tharaud, S. Chat, T. Pellegrino, C. Ménager, F. Gazeau and C. Wilhelm, *Biomaterials*, 2014, **35**, 6400.
22 A. F. Craievich, in *In Handbook of Sol-Gel Science and Technology*, ed. S. Sakka, Springer US, Norwell, MA, 2005, vol. 2, ch. 8, pp. 161.
23 A. Jordan, R. Scholz, P. Wust, H. Fähling and F. Roland, *J. Magn. Magn. Mater.*, 1999, **201**, 413.
24 C. Guibert, V. Dupuis, V. Peyre and J. Fresnais, *J. Phys. Chem. C*, 2015, **119**, 28148.
25 C. C. Berry, S. Wells, S. Charles, G. Aitchison and A. S. G. Curtis, *Biomaterials*, 2004, **25**, 5405.
26 J.-H. Lee, K.-J. Chen, S.-H. Noh, M. A. Garcia, H. Wang, W.-Y. Lin, H. Jeong, B. J. Kong, D. B. Stout, J. Cheon and H.-R. Tseng, *Angew. Chem*., 2013, **52**, 4384.